A negative imaginary theory-based time-varying group formation tracking scheme for multi-robot systems: Applications to quadcopters

Authors' Camera Ready Manuscript. To appear in the
Proceedings of the 40th IEEE International Conference on Robotics and Automation, ExCeL London, UK, May 2023,
Please cite using bibliographic data of the associated published version.

A negative imaginary theory-based time-varying group formation tracking scheme for multi-robot systems: Applications to quadcopters

Yu-Hsiang Su, Parijat Bhowmick, *Member, IEEE*, and Alexander Lanzon, *Senior Member, IEEE*

***Abstract*— This paper proposes a new methodology to develop a time-varying group formation tracking scheme for a class of multi-agent systems (e.g. different types of multi-robot systems) utilising Negative Imaginary (NI) theory. It offers a two-loop control scheme in which the inner loop deploys an appropriate feedback linearising control law to transform the nonlinear dynamics of each agent into a double integrator system, while the outer loop applies an NI-based time-varying group formation control protocol on the linearised agents. This approach offers greater flexibility in choosing a controller, easy implementation and tuning, reduces the overall complexity of the scheme, and uses only output feedback (hence reduced sensing requirements) to achieve formation control in contrast to the existing formation control schemes. The paper has also provided lab-based experimental validation results to demonstrate the feasibility and usefulness of the proposed scheme. Two experiments were conducted on a group of small-scale quadcopters connected via a network to test the time-varying group formation tracking performance.**

I. Introduction

Cooperative control of multi-robot systems has gained significant attention from the robotics and control community over the past two decades due to its potential applications in solving a variety of complex and repetitive tasks. For instance, localisation and mapping [1], search, rescue and retrieval operations [2], multi-target enclosing and surveillance [3], cooperative payload transportation [4], [5], etc. The term cooperative control encompasses leader-following consensus control, formation control, rendezvous control, group formation tracking, etc. References [6] and [7] did pioneering work on developing consensus-based static formation control schemes for multi-vehicle systems. Later, [8] and [9] addressed the time-varying formation control problem for different multi-agent systems. However, the formation control strategies discussed so far require full state (i.e. all states) feedback information, which may not always be feasible in practice because of an inability to take sensor measurements from all the states. Instead, an output feedback cooperative control scheme can be a better option when all states cannot be measured.

This work was supported by the Engineering and Physical Sciences Research Council (EPSRC) [grant number EP/R008876/1]. All research data supporting this publication are directly available within this publication. For the purpose of open access, the authors have applied a Creative Commons Attribution (CC BY) licence to any Author Accepted Manuscript version arising.

Y.-H. Su and A. Lanzon are with the Department of EEE, School of Engineering, University of Manchester, Manchester, M13 9PL, UK. and P. Bhowmick is with the Department of EE, IIT Guwahati, Assam - 781039, India. Emails: Yu-Hsiang.Su@manchester.ac.uk, parijat.bhowmick@iitg.ac.in, Alexander.Lanzon@manchester.ac.uk.

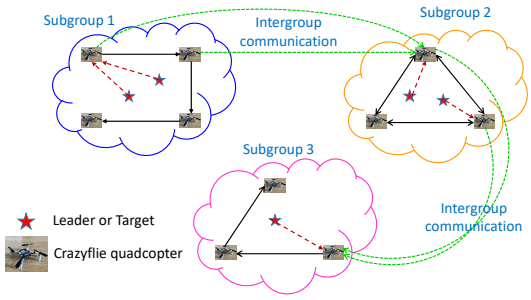

Fig. 1. A typical quadcopter group formation tracking scenario that consists of three subgroups. Each subgroup has attained its respective formation.

Negative Imaginary (NI) systems theory was introduced in 2008 and was inspired by the 'positive position feedback control' of highly resonant mechanical systems [10]. At its inception, NI theory attracted interest of the control community for offering specialised control techniques for vibration attenuation of lightly-damped mechanical systems with colocated input-output pairs (e.g. cantilever beam [10], [11], robotic manipulators [12], etc.). Besides its most renowned application in vibration control, NI theory has also established its worth in solving a variety of engineering problems, such as in nano-positioning applications [13], in vehicle platooning [14], in control of networked multi-agent systems [15], [16], [17], etc. NI theory has become appealing also due to its simple internal stability condition[1] that depends on the loop gain only at the zero frequency and since it offers a stand-alone robust control analysis and synthesis framework [10], [12].

Lately, the NI framework has been utilised as a suitable cooperative control technique for multi-agent systems (MASs) [15], [17], [20], [21]. NI theory is appealing in MAS research because it directly captures the inertial dynamic or kinematic relationships between force or reference velocity actuation and the resulting position [10], [15], [16], [18]. The idea of utilising the NI theory for developing a cooperative control scheme has stemmed from the fact that a particular class of robotic and mechatronic systems can be modelled as a group of networked double/single integrator agents, which inherently satisfies NI property with poles at the origin. Hence, a distributed SNI controller can conveniently stabilise such systems and achieves the desired consensus/formation. Motivated by the applications above, this paper aims to develop a simple yet effective time-varying group formation

[1] A necessary and sufficient condition for the internal stability of a positive feedback interconnection of NI and SNI systems, say $M(s)$ and $N(s)$, is $\lambda_{\max}[N(0)M(0)] < 1$ [10], [18], [19].

tracking (TGFT) scheme for a class of multi-agent systems, including multi-robot systems. A typical group formation tracking scenario involving networked quadcopters has been illustrated in Fig. 1. This paper introduces a new methodology (instead of the commonly used Lyapunov-based approach) to prove the asymptotic convergence of the group formation tracking errors of networked agents by exploiting the unique characteristics of the eigenvalue loci of networked NI and SNI systems. In addition, the proposed NI-based TGFT scheme only requires output feedback and therefore minimises the requirement for sensors and estimators. The feasibility and effectiveness of the proposed scheme are demonstrated via real-time experiments (refer to Fig. 6 and Fig. 8) conducted on a group of networked small-scale quadcopters.

II. Preliminaries and Problem Formulation

A. Negative Imaginary systems theory

Definition 1: (**NI systems**) [12], [18]. Let $M(s)$ be the real, rational and proper transfer function of a square and causal system without any poles in the open right-half plane (RHP). $M(s)$ is said to be Negative Imaginary (NI) if

- $j\left[M(j\omega) - M(j\omega)^*\right] \geq 0$ for all $\omega \in (0, \infty)$ except the values of ω where $s = j\omega$ is a pole of $M(s)$;
- If $s = j\omega_0$ with $\omega_0 \in (0, \infty)$ is a pole of $M(s)$, then it is at most a simple pole and the residue matrix $\lim_{s \to j\omega_0} (s - j\omega_0) jM(s)$ is Hermitian and positive semidefinite;
- If $s = 0$ is a pole of $M(s)$, then the $\lim_{s \to 0} s^k M(s) = 0$ for all $k \geq 3$ and $\lim_{s \to 0} s^2 M(s)$ is Hermitian and positive semidefinite.

Definition 2: (**SNI systems**) [10]. Let $M(s)$ be the real, rational and proper transfer function of a square and causal system. $M(s)$ is said to be Strictly Negative Imaginary if $M(s)$ has no poles in $\{s \in \mathbb{C} : \mathbb{R}[s] \geq 0\}$ and $j\left[M(j\omega) - M(j\omega)^*\right] \geq 0$ for all $\omega \in (0, \infty)$.

B. Graph theory

A group of networked robots exchanges information with each other via an interaction topology. In this work, we use a weighted undirected graph $\mathscr{G} = \{\mathscr{V}, \mathscr{E}, \mathscr{A}\}$ to describe the interaction topology among each robot, where $\mathscr{V} = \{1, ..., m\}$ is the node set, $\mathscr{E} \subset \mathscr{V} \times \mathscr{V}$ is the edge set and $\mathscr{A} = [a_{ij}] \in \mathbb{R}^{m \times m}$ is the associated adjacency matrix respectively. The edge $e_{ji} = (v_j, v_i) \in \mathscr{E}$ denotes the information passes from node j to node i. a_{ij} represents the weight of e_{ji} and $a_{ij} > 0$ if $e_{ji} \in \mathscr{E}$. The in-degree matrix is defined as $\mathscr{D} = \text{diag}\{d_i\} \in \mathbb{R}^{m \times m}$ with $d_i = \sum_{j=1}^{m} a_{ij}$. The Laplacian matrix $\mathscr{L} \in \mathbb{R}^{m \times m}$ of $\mathscr{G}$ is defined as $\mathscr{L} = \mathscr{D} - \mathscr{A}$. If the i^{th} robot is connected to the leader or target (labelled as 'k'), an edge e_{ki} is said to exist between them with a pinning gain $g_i > 0$.

C. Properties of networked NI and SNI systems

Below, we declare the properties of the interaction topology of the networked agents considered in this paper.

Assumption 1: The interaction topology of m agents (in the homogeneous case) is described by an undirected and connected graph $\mathscr{G}$. There always exists a root node (also called the leader or target) which provides reference trajectory to the follower agents (at least to one follower).
According to Assumption 1, we have $(\mathscr{L} + G) > 0$ where $G = \text{diag}\{g_1, g_2, \cdots, g_m\} > 0$ is the pinning-gain matrix. The following lemma proves that a network of homogeneous LTI systems that satisfies Assumption 1 exhibits stable NI (resp. SNI) property if and only if each individual system of the network is stable NI (resp. SNI).

Lemma 1: [21], [22]. Consider a network of N identical stable NI (including SNI) agents that satisfies Assumption 1. Then, $\bar{M}(s) = (\mathscr{L} + G) \otimes M(s)$ is stable NI (resp. SNI) if and only if $M(s) \in \mathscr{RH}_{\infty}^{n \times n}$ is NI (resp. SNI).
Lemma 2 shows that a network of all homogeneous stable NI (including SNI) systems retains the same sign definiteness of its DC-gain matrix when the corresponding interaction topology satisfies Assumption 1.

Lemma 2: [21], [22]. Consider a network of N identical stable NI agents $M(s) \in \mathscr{RH}_{\infty}^{n \times n}$ satisfying Assumption 1. Denote $\bar{M}(s) = (\mathscr{L}+G) \otimes M(s)$. Then, $\bar{M}(0) > 0$ (resp. < 0) if and only if $M(0) > 0$ (resp. < 0).

D. Eigenvalue loci theory

Similar to a Nyquist plot, the eigenvalue loci $\rho_i(s)$ for $i \in \{1, 2, \ldots, n\}$ of a transfer function matrix $G(s)$ is a conformal mapping of the function $\det[G(s)]$ in a complex plane, known as the eigenvalue loci plane, when s traverses along the s-plane D-contour in the clockwise direction as shown in Fig. 4a. For complete details of the eigenvalue loci theory, please see [23], [24].

Theorem 1: [23], [24]. The negative feedback interconnection of a plant $M(s)$ and a controller $N(s)$ is asymptotically stable if and only if the net sum of the critical point $(-1 + j0)$ encirclements of all the eigenvalue loci $\rho_i(jw)$ of the loop transfer function $M(s)N(s)$ for $i \in \{1, 2, \ldots, n\}$ is counter-clockwise and equal to the number of RHP zeros of the open-loop characteristic polynomial. For open-loop stable cases, none of $\rho_i(jw)$ should encircle the critical point $(-1 + j0)$.

E. Problem formulation

Given a multi-robot system that can be modelled as or transformed into a group of networked double integrator agents, the control objective is to first split the agents into several subgroups depending on the locations/positions of the targets (or the leaders) and then design an NI-based time-varying group formation tracking scheme such that each individual subgroup attains the desired static/time-varying formation and keep tracking the static/moving targets assigned to each subgroup.

III. An NI-based time-varying group formation tracking scheme for multi-robot systems

This section lays down the main contribution of this paper, which is developing a time-varying group formation

tracking scheme for a class of multi-agent systems (e.g. a class of multi-robot systems) whose dynamics/kinematics can be approximated by a group of double integrator agents connected via an undirected graph. Note that some subgroups may have multiple targets assigned to them, and the targets may also be time-varying. The proposed TGFT scheme is shown in Fig. 2.

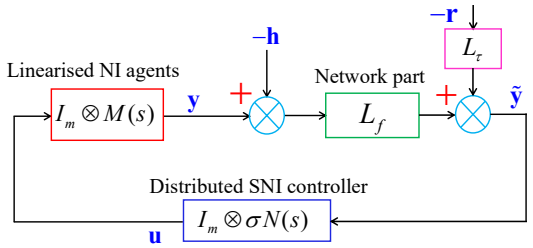

Fig. 2. An NI-based time-varying group formation tracking (TGFT) scheme for a class of multi-agent systems with multiple targets to track.

Consider m agents having transfer function $M(s)$ and τ targets (or leaders). Let the agents be distributed into p subgroups where $p \geq 1$. The node set corresponding to each subgroup is represented by $\mathscr{V}_{\bar{i}}$ for $\bar{i} \in \{1, 2, \ldots, p\}$. Therefore, the total node set $\mathscr{V} = \bigcup_{\bar{i}=1}^{p} \mathscr{V}_{\bar{i}}$. We assume $\mathscr{V}_{\bar{i}} \neq \emptyset$ for any $\bar{i}$ and $\mathscr{V}_k \cap \mathscr{V}_l = \emptyset$ for any $k, l \in \{1, 2, \ldots, p\}$ and $k \neq l$. Each subgroup $\mathscr{V}_{\bar{i}}$ represents a part of the whole graph $\mathscr{G}$, designated by $\mathscr{G}_{\bar{i}}$. Suppose the $\bar{i}^{\text{th}}$ subgroup $\mathscr{V}_{\bar{i}}$ has $m_{\bar{i}}$ agents (i.e. nodes in terms of graph theory) satisfying $\sum_{\bar{i}=1}^{p} m_{\bar{i}} = m$ and it has $\tau_{\bar{i}} \geq 1$ targets (or leaders) assigned to it such that $\sum_{\bar{i}=1}^{p} \tau_{\bar{i}} = \tau$. The Laplacian matrix of the whole network is given by $\mathscr{L} = \left[\begin{array}{c|c} \mathscr{L}_f & \mathscr{L}_\tau \\ \hline 0 & 0 \end{array}\right]$ where $\mathscr{L}_f \in \mathbb{R}^{m \times m}$ is the Laplacian matrix of the follower agents and $\mathscr{L}_\tau \in \mathbb{R}^{m \times \tau}$ is the Laplacian matrix that connects the target nodes (or the leaders) to the follower agents. Below, we declare some important assumptions to be satisfied by the networked multi-agent systems considered in this paper.

Assumption 2: The node subsets $\{\mathscr{V}_1, \mathscr{V}_2, \cdots, \mathscr{V}_p\}$ do not form any cycle among them. This ensures that the intergroup communication will be directed, that is, no cycle will exist among the subgroups.

This assumption results in a particular structure of $\mathscr{L}_f$ as

$$\mathscr{L}_f = \begin{bmatrix} \mathscr{L}_{11} & 0 & \cdots & 0 \\ \mathscr{L}_{21} & \mathscr{L}_{22} & \cdots & 0 \\ \vdots & \vdots & \ddots & \vdots \\ \mathscr{L}_{p1} & \mathscr{L}_{p2} & \cdots & \mathscr{L}_{pp} \end{bmatrix}. \tag{1}$$

For an undirected graph, $\mathscr{L}_{\bar{i}\bar{i}} > 0$ and for directed cases, $\mathscr{L}_{\bar{i}\bar{i}}$ satisfies the properties of an M-matrix when each subgroup contains a spanning tree.

Assumption 3: The row-sum of each of the rows of the sub-Laplacian matrices $\mathscr{L}_{\bar{i}\bar{j}}$ where $\bar{i}, \bar{j} \in \{1, 2, \ldots, p\}$ is zero when $\bar{i} > \bar{j}$.

Lemma 3: [25] For an undirected or directed graph satisfying Assumptions 2 and 3, as described before,

$$-\mathscr{L}_f^{-1}\mathscr{L}_\tau = \text{diag}\left\{\boldsymbol{\eta}_1, \boldsymbol{\eta}_2, \cdots, \boldsymbol{\eta}_p\right\} \tag{2}$$

where $\boldsymbol{\eta}_{\bar{i}} = \mathbf{1}_{m_{\bar{i}}}\left[g_1^{(\bar{i})}, g_2^{(\bar{i})}, \cdots, g_{\tau_{\bar{i}}}^{(\bar{i})}\right] / \sum_{k=1}^{\tau_{\bar{i}}} g_k^{(\bar{i})}$. $g_k^{(\bar{i})}$ denotes the weights of the edges that connect the target nodes (or the leaders) to the follower agents belonging to the $\bar{i}^{\text{th}}$ subgroup for $\bar{i} \in \{1, 2, \ldots, p\}$.

Theorem 2: Consider a homogeneous multi-agent system consisting of m agents and τ targets. The model of the agent has been feedback-linearised into or approximated by $M(s) = \frac{1}{s^2}$. Suppose the agents are split into p ($p \geq 1$) subgroups $\{\mathscr{V}_1, \mathscr{V}_2, \cdots, \mathscr{V}_p\}$, each of which contains $m_{\bar{i}}$ agents and has been assigned $\tau_{\bar{i}}$ targets (or leaders) to track. Let Assumption 1 hold for each subgroup $\mathscr{V}_{\bar{i}}$ along with Assumptions 2 and 3. Choose an SNI transfer function $N(s) \in \mathscr{RH}_\infty$ with $N(0) < 0$. Then, the network of linearised double integrator agents achieves time-varying group formation tracking by the following output feedback distributed SNI control law (according to the scheme shown in Fig. 2)

$$u_i = \sigma N(s)\Bigg[\sum_{j=1}^{m} a_{ij}\big((y_i - h_i) - (y_j - h_j)\big) + \sum_{k=1}^{\tau} a_{ik}(y_i - h_i - r_k)\Bigg] \tag{3}$$

$\forall i \in \{1, 2, \ldots, m\}$ and for any $\sigma \in (0, \infty)$.

Proof. We will now introduce a set of notations that will be used in this proof. Let $\bar{\mathbf{r}}_{\bar{i}}(t)$ and $\bar{\mathbf{h}}_{\bar{i}}(t)$ denote respectively the formation reference and formation configuration vectors for the $\bar{i}^{\text{th}}$ subgroup where $\bar{i} \in \{1, 2, \ldots, p\}$. It can be readily shown that $\mathbf{r}(t) = [r_1, r_2, \cdots, r_m]^\top = [\bar{\mathbf{r}}_1^\top, \bar{\mathbf{r}}_2^\top, \cdots \bar{\mathbf{r}}_p^\top]^\top$ and $\mathbf{h}(t) = [h_1, h_2, \cdots, h_m]^\top = [\bar{\mathbf{h}}_1^\top, \bar{\mathbf{h}}_2^\top, \cdots \bar{\mathbf{h}}_p^\top]^\top$. The output vector of each subgroup is denoted by $\bar{\mathbf{y}}_{\bar{\mathbf{i}}}$ and hence, the global output vector $\mathbf{y} = [y_1, y_2, \cdots, y_m]^\top = [\bar{\mathbf{y}}_1^\top, \bar{\mathbf{y}}_2^\top, \cdots \bar{\mathbf{y}}_p^\top]^\top$.

The proof has been divided into two parts. **Part I** establishes the asymptotic stability of the entire networked closed-loop system shown in Fig. 2, and **Part II** shows that the group formation tracking error for each agent asymptotically decays to zero.

The control law u_i given in (3) can be rearranged to express the group-wise control law vector

$$\bar{\mathbf{u}}_{\bar{i}} = \sigma N(s)\big[\mathscr{L}_{\bar{i}\bar{i}}(\bar{\mathbf{y}}_{\bar{i}} - \bar{\mathbf{h}}_{\bar{i}}) + \mathscr{L}_{\bar{i}\bar{j}}(\bar{\mathbf{y}}_{\bar{j}} - \bar{\mathbf{h}}_{\bar{j}}) - \mathscr{L}_{\tau_{\bar{i}}}\bar{\mathbf{r}}_{\bar{i}}\big] \tag{4}$$

where $\bar{i}, \bar{j} \in \{1, 2, \ldots, p\}$. Following (4), Fig. 2 has been redrawn in Fig. 3 that shows the formation tracking module for each subgroup.

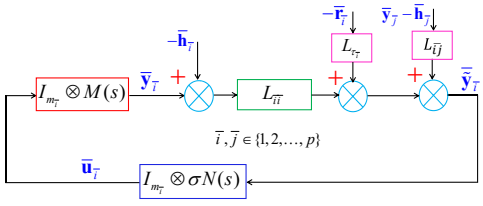

Fig. 3. The underlying formation tracking scheme for each subgroup. All such subgroups together form the complete TGFT scheme shown in Fig. 2.

Now the stability of the entire closed-loop networked system shown in Fig. 2 can be guaranteed if each subgroup (shown in Fig. 3) remains asymptotically stable on noting that both $\bar{\mathbf{r}}_{\bar{i}} \in \mathscr{L}_\infty^{m_{\bar{i}}}$ and $\bar{\mathbf{h}}_{\bar{i}} \in \mathscr{L}_\infty^{m_{\bar{i}}}$ are smooth signals.

Part I – Closed-loop stability of each subgroup: In this part, the notation $\bar{\rho}_i(s)$, for $i \in \{1, 2, \ldots, m_{\bar{i}}\}$, denotes the eigenvalue loci of the loop transfer function matrix of the $\bar{i}^{\text{th}}$ subgroup $[\mathscr{L}_{\bar{i}\bar{i}} \otimes \frac{1}{s^2} N(s)]$. For convenience, we will define the following three sets of the complex variable s along the s-plane D-contour shown in Fig. 4a:

$$\Omega_0 = \{s|\ s = \varepsilon e^{j\theta},\ \varepsilon \in \mathbb{R}_{>0},\ \varepsilon \to 0_+,\ -\frac{\pi}{2} \le \theta \le \frac{\pi}{2}\},$$
$$\Omega_{\pm j} = \{s|\ s = j\omega,\ \omega \in (-\infty, 0) \cup (0, \infty)\},$$
$$\Omega_R = \{s|\ s = Re^{j\theta},\ R \in \mathbb{R}_{>0}, R \to +\infty,\ -\frac{\pi}{2} \le \theta \le \frac{\pi}{2}\}.$$

The positive feedback interconnection of $[\mathscr{L}_{\bar{i}\bar{i}} \otimes N(s)]$ and $\left(I_{m_{\bar{i}}} \otimes \frac{\sigma}{s^2}\right)$, as shown in Fig. 3, remains asymptotically stable for all $\sigma \in (0, \infty)$ if none of the eigenvalue loci $\bar{\rho}_i(j\omega)$ encircles the critical point $(\frac{1}{\sigma} + j0)$ via Theorem 1.

Case I: When $s \in \Omega_0$ The eigenvalue loci $\bar{\rho}_i(s)$ can approximately be expressed as

$$\bar{\rho}_i(s)|_{s\in\Omega_0} \simeq \lambda_i\left[\mathscr{L}_{\bar{i}\bar{i}} \otimes N(0)\right] \frac{1}{\varepsilon^2} e^{-j2\theta} \tag{6}$$

$\forall i \in \{1, 2, \ldots, m_{\bar{i}}\}$, which can be further simplified as $\bar{\rho}_i(s)|_{s\in\Omega_0} \simeq \frac{c_i}{\varepsilon^2} e^{j(\phi_i - 2\theta)}$ on setting $\lambda_i\left[\mathscr{L}_{\bar{i}\bar{i}} \otimes N(0)\right] = c_i e^{j\phi_i}$ where $\phi_i = -\pi\ \forall i$ as $N(0) < 0$ and $\mathscr{L}_{\bar{i}\bar{i}} > 0$. Therefore, $\bar{\rho}_i(j0_+) \simeq \frac{c_i}{\varepsilon^2} e^{-j2\pi} \to +\infty\angle -2\pi$ as $\varepsilon \to 0_+$ and when $\theta = \frac{\pi}{2}$. It is essential to note[2] here that $\angle\bar{\rho}_i(j0_+) \gtrsim -2\pi$ since $\angle\gamma(j0_+) \gtrsim -\pi$. Similarly, $\bar{\rho}_i(j0_-) \to +\infty\angle 0$ with $\angle\bar{\rho}_i(j0_-) \lesssim 0$. This implies $-2\pi \lesssim \angle\bar{\rho}_i(j\omega) \lesssim 0$ when $s \in \Omega_0$. Hence, no infinite crossover takes place on the positive real axis when each eigenvalue locus $\bar{\rho}_i(j\omega)$ encloses the zero-frequency points $\bar{\rho}_i(j0_-)$ and $\bar{\rho}_i(j0_+)$ via a semicircular arc of infinite radius in the clockwise direction as illustrated in Fig. 4b.

Case II: When $s \in \Omega_{\pm j}$ Let $\lambda_i\left[\mathscr{L}_{\bar{i}\bar{i}} \otimes N(j\omega)\right] = c_i e^{j\phi_i}$ at each $\omega \in (0, \infty)$ and for all $i \in \{1, 2, \ldots, m_{\bar{i}}\}$. Since $N(s)$ is SNI, $\phi_i(\omega) \in (-\pi, 0)\ \forall\omega \in (0, \infty)$ and hence, $\angle\bar{\rho}_i(j\omega) = (\phi_i - \pi) \in (-2\pi, -\pi]\ \forall\omega \in (0, \infty)$ and $\forall i$. Similarly, for all $\omega \in (-\infty, 0)$, $\angle\bar{\rho}_i(j\omega) \in [-\pi, 0)$. Therefore, when $s \in \Omega_{\pm j}$, all $\bar{\rho}_i(j\omega)$ stay within the Green coloured region (shown in Fig. 4b) of the eigenvalue loci plane without touching anywhere on the positive real axis.

Case III: When $s \in \Omega_R$ For $s \in \Omega_R$, the eigenvalue loci $\bar{\rho}_i(s)$ where $i \in \{1, 2, \ldots, m_{\bar{i}}\}$ can be expressed as

$$\bar{\rho}_i(s)|_{s\in\Omega_R} \simeq \lambda_i\left[\mathscr{L}_{\bar{i}\bar{i}} \otimes N(\infty)\right] \frac{e^{-j2\theta}}{R^2} = \frac{c_i}{R^2} e^{j(\phi_i - 2\theta)}$$

upon denoting $\lambda_i\left[\mathscr{L}_{\bar{i}\bar{i}} \otimes N(\infty)\right] = c_i e^{j\phi_i}$. Note that $\phi_i = -\pi$ for all i as $N(\infty) < 0$ owing to $N(s)$ being SNI with $N(0) < 0$. Therefore, $\bar{\rho}_i(+j\infty) \simeq \frac{c_i}{R^2} e^{-j\frac{3\pi}{2}} \to 0\angle -\frac{3\pi}{2}$ and $\bar{\rho}_i(-j\infty) \to 0\angle -\frac{\pi}{2}$. This then follows that each $\bar{\rho}_i(j\omega)$ encloses the points $\bar{\rho}_i(+j\infty)$ and $\bar{\rho}_i(-j\infty)$ through a semicircular arc (i.e. the Orange coloured arc around the origin shown in Fig. 4b) of infinitesimal radius in the counter-clockwise direction.

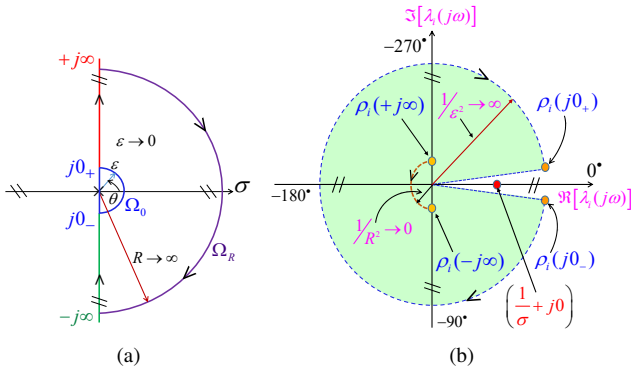

Fig. 4. (a) Nyquist $\mathscr{D}$-contour in the s-plane; and (b) All the eigenvalue loci $\bar{\rho}_i(j\omega)$ of $\mathscr{L}_{\bar{i}\bar{i}} \otimes \frac{1}{s^2} N(s)$ remain confined within the Green coloured region $\forall\omega \in \mathbb{R} \cup \{\infty\}$ when $N(s)$ is SNI having $N(0) < 0$.

Cases I, II and III together prove that all the eigenvalue loci $\bar{\rho}_i(s)$ remain within the Green coloured region shown in Fig. 4b and hence, none of $\bar{\rho}_i(s)$ encircles the critical point $(\frac{1}{\sigma} + j0)$ for any $\sigma \in (0, \infty)$. This proves asymptotic stability of the $\bar{i}^{\text{th}}$ subgroup for all $\bar{i}$ exploiting Theorem 1. Applying this result, we can conclude that all subgroups are asymptotically stable, which ultimately implies asymptotic stability of the scheme shown in Fig. 2.

Part II – Group formation tracking: The global group formation tracking error vector can be constructed from (3) as $\boldsymbol{\Xi} = [\xi_1, \xi_2, \cdots, \xi_m]^\top = \mathscr{L}_f(\mathbf{y} - \mathbf{h}) + \mathscr{L}_\tau \mathbf{r}$. Since the networked system is asymptotically stable, $\lim_{t\to\infty} \boldsymbol{\Xi}(t) = 0$. It implies $\lim_{t\to\infty} \left(\mathbf{y}(t) - \mathbf{h}(t) - \mathscr{L}_f^{-1}\mathscr{L}_\tau \mathbf{r}(t)\right) = \mathbf{0}$ which in turn implies $\lim_{t\to\infty} \left(\mathbf{y}(t) - \mathbf{h}(t) - \text{diag}\left\{\boldsymbol{\eta}_1, \boldsymbol{\eta}_2, \cdots, \boldsymbol{\eta}_p\right\} \mathbf{r}(t)\right) = \mathbf{0}$ via Lemma 3. The last expression is equivalent to $\lim_{t\to\infty} \begin{bmatrix} \bar{\mathbf{y}}_1(t) - \bar{\mathbf{h}}_1(t) - \boldsymbol{\eta}_1\bar{\mathbf{r}}_1(t) \\ \bar{\mathbf{y}}_2(t) - \bar{\mathbf{h}}_2(t) - \boldsymbol{\eta}_2\bar{\mathbf{r}}_2(t) \\ \vdots \\ \bar{\mathbf{y}}_p(t) - \bar{\mathbf{h}}_p(t) - \boldsymbol{\eta}_p\bar{\mathbf{r}}_p(t) \end{bmatrix} = \mathbf{0}$. This can be rearranged into the following elegant expression

$$\lim_{t\to\infty} \left[\bar{\mathbf{y}}_{\bar{i}}(t) - \bar{\mathbf{h}}_{\bar{i}}(t) - \mathbf{1}_{m_{\bar{i}}} \sum_{k=1}^{\tau_{\bar{i}}} \frac{g_k^{(\bar{i})}}{\sum_{j=1}^{\tau_{\bar{i}}} g_j^{(\bar{i})}} r_k(t)\right] = \mathbf{0} \tag{7}$$

for all $\bar{i} \in \{1, 2, \ldots, p\}$. This hence proves that each subgroup will asymptotically attain the desired sub-formation specified by $\bar{\mathbf{h}}_{\bar{i}}$. It is crucial here to note that $\sum_{k=1}^{\tau_{\bar{i}}} \frac{g_k^{(\bar{i})}}{\sum_{j=1}^{\tau_{\bar{i}}} g_j^{(\bar{i})}} = 1$, which implies that each subgroup formation assembly keeps tracking a convex combination of the targets (or leaders). ■

[2] $\gamma_k(s)$ denotes the eigenvalue loci of $N(s)$ for each $k \in \{1, 2, \ldots, m_{\bar{i}}\}$. When $N(s)$ is SNI with $N(0) < 0$, $\angle\gamma_k(j0_+) \gtrsim -\pi$ for all k since $\lim_{\omega\to 0} \frac{\mathrm{d}}{\mathrm{d}\omega}\angle\gamma_k(j\omega) < 0$ for all k. The symbols $\gtrsim$ and $\lesssim$ denote respectively the relational operations 'slightly greater than' and 'slightly lesser than'.

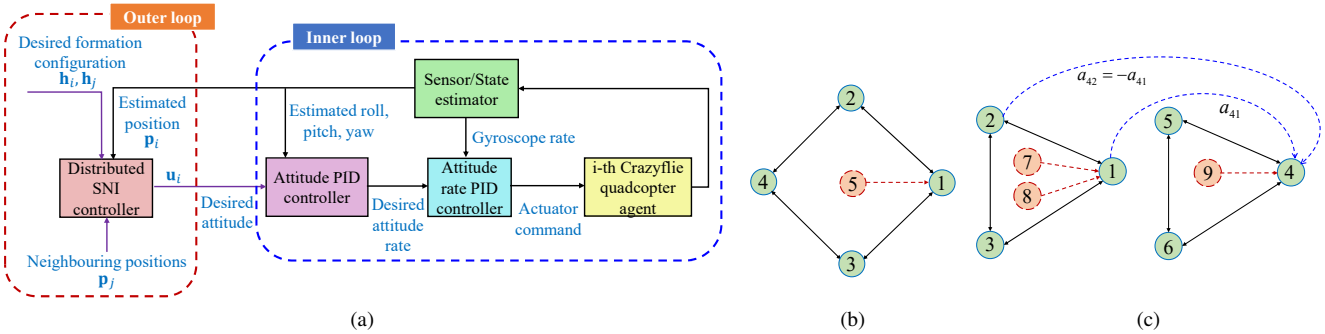

Fig. 5. (a) The proposed two-loop hardware control configuration for quadcopters to achieve time-varying group formation tracking; (b) Topology 1 connects a group of four quadcopters; (c) Topology 2 shows two subgroups, each of which contains three quadcopters. Dotted red nodes represent virtual targets.

IV. Experimental Validation Results

To validate the feasibility and effectiveness of the proposed NI-based time-varying group formation tracking scheme, we implemented it on a group of Crazyflie 2.1 nano quadcopters [26] connected via a network and conducted two real-time flight experiments. The experiments demonstrate two potential applications: multi-target surveillance and multi-target enclosing tasks with dynamically-varying targets (or leaders). The Loco Positioning system [26] provides the absolute position of each quadcopter with an accuracy of $0.1\,\mathrm{m}$. Fig. 5a presents the two-loop hardware control configuration used in the real-time flight experiments. The inner loop deploys two embedded PID controllers designed such that the closed-loop translational dynamics of a quadcopter become a double integrator. While the distributed SNI controller acts as the outer-loop control scheme and operates on the inner-loop double integrator dynamics. The position information of each quadcopter agent is transmitted to the base station, and the control command is generated through the base station and sent to each agent via Crazyradio dongles [26]. However, the base station can be removed if each quadcopter can sense the relative positions of the neighbouring agents or directly share them via Bluetooth or Wi-fi since the proposed control scheme is fully distributed. The recorded video clips of two real-time flight experiments can be found in the Supplementary Material.

A. Modelling of the quadcopter UAVs

Let $\mathbf{p} = [x, y, z]^\top$, $\boldsymbol{\omega} = [p, q, r]^\top$ and $\boldsymbol{\eta} = [\phi, \theta, \psi]^\top$ be the position vector in the earth frame, the angular velocity vector in the body frame and the Euler angles respectively. m and $\mathbf{I}$ denote the centre of mass of the quadcopter UAV and the inertia matrix. According to Newton-Euler equations, the dynamics of a quadcopter UAV are

$$\begin{cases} m\ddot{\mathbf{p}} = -mg\mathbf{e}_z + \mathbf{R}_e^b(\boldsymbol{\eta})\mathbf{F}_b, \\ \mathbf{I}\dot{\boldsymbol{\omega}} = -\boldsymbol{\omega} \times \mathbf{I}\boldsymbol{\omega} + \boldsymbol{\tau}_b, \end{cases} \tag{8}$$

where g is the gravity constant, $\mathbf{e}_z = [0, 0, 1]^\top$ is the unit vector w.r.t. the earth frame, $\mathbf{R}_e^b(\boldsymbol{\eta})$ is the rotation matrix from the body frame to the earth frame, $\mathbf{F}_b$ is the total force (w.r.t. the body frame) from the rotors and $\boldsymbol{\tau}_b$ is the total drag torque (w.r.t. the body frame) produced by the rotors.

Remark 1: Since the attitude dynamics of a quadcopter UAV are much faster than the translational dynamics, hovering and manoeuvring can be controlled together by a two-loop control scheme shown in Fig. 5a (see [27] and references therein). The outer-loop cooperative control law drives the quadcopters to achieve the desired formations and keep tracking the targets, while the inner-loop control stabilises the attitude dynamics. As a result, the closed-loop translational dynamics of a quadcopter UAV can be approximated by a double integrator system $\ddot{\mathbf{p}}_i = \mathbf{u}_i$, where $\mathbf{p}_i = [x_i, y_i, z_i]^\top$ and $\mathbf{u}_i = [u_{xi}, u_{yi}, u_{zi}]^\top$ denote respectively the position and control input vectors (i.e. the desired acceleration) of the i^{th} quadcopter UAV. For more details on the quadcopter UAV modelling part, the article [28] may be referred.

B. Experiment 1: Time-varying formation tracking mission

In Experiment 1, four Crazyflie quadcopters are used to perform a time-varying formation tracking mission. In the first $25\,\mathrm{s}$, four quadcopters are expected to achieve a time-varying circular formation surrounding the static virtual target. After $25\,\mathrm{s}$, four quadcopters should track the moving virtual target while maintaining the time-varying circular formation. Fig. 5b describes the interaction topology between all quadcopters and the virtual target. The time-varying circular formation in the X and Y directions for the four quadcopters is given by

$$\mathbf{h}_i(t) = \begin{bmatrix} \cos\left(0.02t + \frac{2(i-1)\pi}{4}\right) \\ \sin\left(0.02t + \frac{2(i-1)\pi}{4}\right) \end{bmatrix} \quad \forall i \in \{1, 2, ..., 4\}.$$

In addition, we chose an SNI controller $N(s) = -\frac{s+1}{s+10}$, and $\sigma = 20$ for the experiment.

Fig. 6 indicates that four quadcopters achieve the time-varying circular formation while tracking the static/moving virtual target. In addition, Fig. 7a plots the trajectories of all quadcopters and the virtual target, and Fig. 7b shows that the 2-norm of the formation error of each quadcopter converges to nearly zero after a few seconds. The results validate that four quadcopters achieved the time-varying formation tracking mission via the proposed NI-based TGFT scheme.

C. Experiment 2: Time-varying group formation mission

In Experiment 2, six Crazyflie quadcopters are used to perform a time-varying group formation mission. We assume

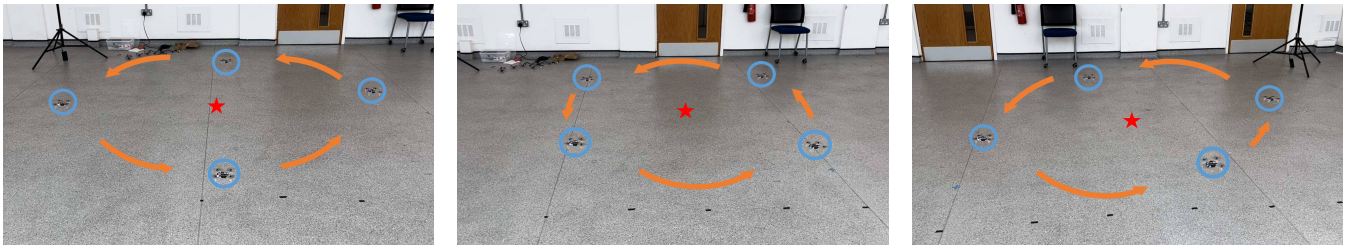

(a) $t = 15\,\mathrm{s}$ (b) $t = 35\,\mathrm{s}$ (c) $t = 40\,\mathrm{s}$

Fig. 6. Snapshots of Experiment 1 at time instants $t = 15\,\mathrm{s}$, $t = 35\,\mathrm{s}$ and $t = 40\,\mathrm{s}$. The red stars mark the positions of the virtual target. (a) At $t = 15\,\mathrm{s}$, all quadcopters achieve a time-varying circular formation surrounding the static virtual target; (b) At $t = 35\,\mathrm{s}$, all quadcopters maintain a time-varying circular formation while tracking the moving virtual target; (c) At $t = 40\,\mathrm{s}$, all quadcopters reach the final positions, and the mission is complete.

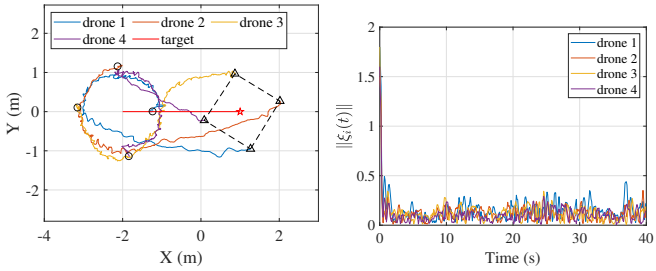

(a) (b)

Fig. 7. (a) Trajectories of all quadcopters in the X-Y plane of Experiment 1. The circles mark the initial positions, and the triangles mark the final positions of all quadcopters, respectively. The red star marks the final position of the moving virtual target; (b) The 2-norm of the formation error $\|\xi_i(t)\|$ of each quadcopter of Experiment 1.

that there are three virtual targets to be monitored. Fig. 5c describes the interaction topology between all quadcopters and three virtual targets. Six quadcopters are divided into two subgroups depending on their relative positions to the virtual targets to form an individual sub-formation around each virtual target. One subgroup is expected to build a time-varying circular formation around two virtual targets, while the other should surround one virtual target. The time-varying circular formation in the X and Y directions for the six quadcopters is given by

$$\mathbf{h}_i(t) = \begin{bmatrix} \cos\left(0.02t + \frac{2(i-1)\pi}{3}\right) \\ \sin\left(0.02t + \frac{2(i-1)\pi}{3}\right) \end{bmatrix} \quad \forall i \in \{1, 2, ..., 6\}.$$

Here, we chose the same SNI controller $N(s) = -\frac{s+1}{s+10}$, and $\sigma = 20$ as experiment 1.

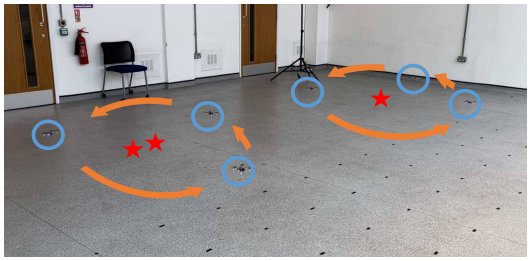

Fig. 8. A snapshot of the time-varying group formation mission during Experiment 2. The red stars mark the positions of three virtual targets.

Fig. 8 indicates that the subgroup on the left achieves the circular time-varying formation surrounding two virtual targets, and the subgroup on the right achieves the circular time-varying formation surrounding one virtual target. In addition, Fig. 9a plots the trajectories of all quadcopters and the positions of three virtual targets, while Fig. 9b shows that the 2-norm of the formation error of each quadcopter converges to nearly zero after a few seconds. The results validate that six quadcopters achieved the time-varying group formation mission via the proposed NI-based TGFT scheme.

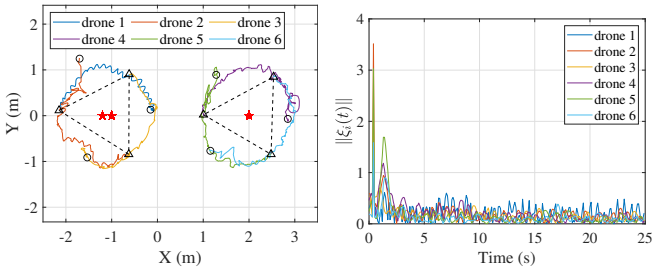

(a) (b)

Fig. 9. (a) Trajectories of all quadcopters in the X-Y plane of Experiment 2. The circles mark the initial positions, and the triangles mark the final positions of all quadcopters, respectively. The red stars mark the positions of three virtual targets; (b) The 2-norm of the formation error $\|\xi_i(t)\|$ of each quadcopter of Experiment 2.

V. Conclusions

This paper has exploited NI theory to propose a novel time-varying group formation tracking scheme for multi-robot systems that can be modelled as or transformed into a group of networked double integrator agents. Compared to conventional formation controllers that use full state feedback information and the Lyapunov stability approach, the proposed methodology only requires output feedback (hence a reduced number of sensors), and the asymptotic convergence of the group formation tracking error is proven by the eigenvalue loci technique. Finally, two real-time flight experiments were conducted on small-scale quadcopters to validate the effectiveness and feasibility of the proposed NI-based time-varying group formation tracking scheme and showcase its usefulness in practice.

REFERENCES

[1] K. N. McGuire, C. De Wagter, K. Tuyls, H. J. Kappen, and G. C. H. E. de Croon, "Minimal navigation solution for a swarm of tiny flying robots to explore an unknown environment," *Science Robotics*, vol. 4, no. 35, Oct 2019.

[2] J. Hu, P. Bhowmick, I. Jang, F. Arvin, and A. Lanzon, "A decentralized cluster formation containment framework for multirobot systems," *IEEE Transactions on Robotics*, vol. 37, no. 6, pp. 1936–1955, May 2021.

[3] J. Hu, H. Niu, J. Carrasco, B. Lennox, and F. Arvin, "Fault-tolerant cooperative navigation of networked UAV swarms for forest fire monitoring," *Aerospace Science and Technology*, vol. 123, no. 107494, pp. 1–12, April 2022.

[4] H. G. d. Marina and E. Smeur, "Flexible collaborative transportation by a team of rotorcraft," in *Proceedings of the IEEE International Conference on Robotics and Automation*, Montreal, Canada, May 2019, pp. 1074–1080.

[5] G. A. Cardona, M. Arevalo-Castiblanco, D. Tellez-Castro, J. Calderon, and E. Mojica-Nava, "Robust adaptive synchronization of interconnected heterogeneous quadrotors transporting a cable-suspended load," in *Proceedings of the IEEE International Conference on Robotics and Automation*, Xi'an, China, May 2021, pp. 31–37.

[6] W. Ren, R. W. Beard, and E. M. Atkins, "Information consensus in multivehicle cooperative control," *IEEE Control Systems Magazine*, vol. 27, no. 2, pp. 71–82, April 2007.

[7] W. Ren and R. W. Beard, *Distributed Consensus in Multi-vehicle Cooperative Control*, ser. Communications and Control Engineering. London: Springer London, 2008.

[8] X. Dong, B. Yu, Z. Shi, and Y. Zhong, "Time-varying formation control for unmanned aerial vehicles: theories and applications," *IEEE Transactions on Control Systems Technology*, vol. 23, no. 1, pp. 340–348, Jan 2015.

[9] X. Dong, Y. Zhou, Z. Ren, and Y. Zhong, "Time-varying formation tracking for second-order multi-agent systems subjected to switching topologies with application to quadrotor formation flying," *IEEE Transactions on Industrial Electronics*, vol. 64, no. 6, pp. 5014–5024, June 2017.

[10] A. Lanzon and I. R. Petersen, "Stability robustness of a feedback interconnection of systems with negative imaginary frequency response," *IEEE Transactions on Automatic Control*, vol. 53, no. 4, pp. 1042–1046, May 2008.

[11] B. Bhikkaji, S. O. Reza Moheimani, and I. R. Petersen, "A negative imaginary approach to modeling and control of a collocated structure," *IEEE/ASME Transactions on Mechatronics*, vol. 17, no. 4, pp. 717–727, Aug 2012.

[12] M. A. Mabrok, A. G. Kallapur, I. R. Petersen, and A. Lanzon, "Generalizing negative imaginary systems theory to include free body dynamics: Control of highly resonant structures with free body motion," *IEEE Transactions on Automatic Control*, vol. 59, no. 10, pp. 2692–2707, Oct 2014.

[13] S. K. Das, H. R. Pota, and I. R. Petersen, "Resonant controller design for a piezoelectric tube scanner: A 'mixed' negative-imaginary and small-gain approach," *IEEE Transactions on Control Systems Technology*, vol. 22, no. 5, pp. 1899–1906, 2014.

[14] C. Cai and G. Hagen, "Stability analysis for a string of coupled stable subsystems with negative imaginary frequency response," *IEEE Transactions on Automatic Control*, vol. 55, no. 8, pp. 1958–1963, Aug 2010.

[15] J. Wang, A. Lanzon, and I. R. Petersen, "Robust output feedback consensus for networked negative-imaginary systems," *IEEE Transactions on Automatic Control*, vol. 60, no. 9, pp. 2547–2552, Sep 2015.

[16] J. Wang, A. Lanzon, and I. R. Petersen, "Robust cooperative control of multiple heterogeneous negative-imaginary systems," *Automatica*, vol. 61, pp. 64–72, 2015.

[17] O. Skeik, J. Hu, F. Arvin, and A. Lanzon, "Cooperative control of integrator negative imaginary systems with application to rendezvous multiple mobile robots," in *Proceedings of 12th International Workshop on Robot Motion and Control*, Poznan, Poland, July 2019, pp. 15–20.

[18] A. Lanzon and H.-J. Chen, "Feedback stability of negative imaginary systems," *IEEE Transactions on Automatic Control*, vol. 62, no. 11, pp. 5620–5633, Nov 2017.

[19] A. Lanzon and P. Bhowmick, "Characterization of input-output negative imaginary systems in a dissipative framework," *IEEE Transactions on Automatic Control*, vol. 68, no. 2, pp. 959–974, Feb 2023.

[20] V. P. Tran, M. A. Garratt, and I. R. Petersen, "Multi-vehicle formation control and obstacle avoidance using negative-imaginary systems theory," *IFAC Journal of Systems and Control*, vol. 15, no. 100117, pp. 1–23, March 2021.

[21] J. Hu, B. Lennox, and F. Arvin, "Robust formation control for networked robotic systems using negative imaginary dynamics," *Automatica*, vol. 140, no. 110235, pp. 1–9, June 2022.

[22] P. Bhowmick and S. Patra, "On decentralized integral controllability of stable negative-imaginary systems and some related extensions," *Automatica*, vol. 94, pp. 443–451, Aug 2018.

[23] J. J. Belletrutti and A. G. J. MacFarlane, "Characteristic loci techniques in multivariable-control-system design," *Proceedings of the Institution of Electrical Engineers*, vol. 118, no. 9, pp. 1291–1297, Sep 1971.

[24] A. G. J. Macfarlane and J. J. Belletrutti, "The characteristic locus design method," *Automatica*, vol. 9, no. 5, pp. 575–588, 1973.

[25] Z. Li and Z. Duan, *Cooperative control of multi-agent systems: A consensus region approach*, 1st ed. CRC Press, 2014.

[26] Bitcraze, "https://www.bitcraze.io."

[27] Y.-H. Su and A. Lanzon, "Formation-containment tracking and scaling for multiple quadcopters with an application to choke-point navigation," in *Proceedings of the IEEE International Conference on Robotics and Automation*, May 2022, pp. 4908–4914.

[28] D. Mellinger, N. Michael, and V. Kumar, "Trajectory generation and control for precise aggressive maneuvers with quadrotors," *International Journal of Robotics Research*, vol. 31, no. 5, pp. 664–674, 2012.